CONF-860605--6

Radiation-Induced Segregation and Precipitation in Molybdenum-Rhenium Alloys*

CONF-860605--6

DE86 007521

R. A. Erck[1], C. M. Wayman[2] and L. E. Rehn[1]

[1]Materials Science and Technology Division
Argonne National Laboratory
Argonne, IL 60439

[2]Department of Metallurgy and Mining Engineering
University of Illinois
Urbana, IL 61801

February 1986

DISCLAIMER

Submitted to: The Thirteenth International Symposium on the Effects of Radiation on Materials, June 23-25, 1986, Seattle, Washington.

*Work supported by the U. S. Department of Energy, BES-Materials Sciences, under Contract W-31-109-Eng-38.

Radiation-Induced Segregation and Precipitation in Molybdenum-Rhenium Alloys*

R. A. Erck[1], C. M. Wayman[2] and L. E. Rehn[1]

[1]Materials Science and Technology Division
Argonne National Laboratory
Argonne, IL 60439

[2]Department of Metallurgy and Mining Engineering
University of Illinois
Urbana, IL 61801

February 1986

Submitted to: The Thirteenth International Symposium on the Effects of Radiation on Materials, June 23-25, 1986, Seattle, Washington.

*Work supported by the U. S. Department of Energy, BES-Materials Sciences, under Contract W-31-109-Eng-38.

Radiation-Induced Segregation and Precipitation in Molybdenum-Rhenium Alloys*

R. A. Erck[1], C. M. Wayman[2] and L. E. Rehn[1]

Abstract

Specimens of Mo-7 at. % Re and Mo-30 at. % Re were irradiated with 1.8 MeV $^4He^+$ ions at elevated temperatures. Radiation-induced segregation of Re was measured during irradiation by in situ Rutherford backscattering spectrometry. Segregation of the undersized Re atoms in the same direction as the defect fluxes, i.e. toward the external surface, was observed. The amount of Re enrichment in the near-surface region was measured as a function of temperature and of dose at a calculated near-surface displacement rate near 1×10^{-4}dpa/s. Segregation was observed at temperatures from 800°C to 1500°C in Mo-7Re, and from 850°C to 1225°C in Mo-30Re.

Irradiated disks were examined by transmission electron microscopy. Precipitates of Chi phase were observed on grain boundaries, or in a thin layer at the irradiated surface in Mo-30Re after irradiation at temperatures from 750°C to 1075°C. Frequently, Chi precipitates formed with a crystallographic twin orientation with respect to the host matrix. No voids were observed for doses up to 1.6 dpa.

Key Words

ion-irradiation, radiation-induced precipitation, radiation-induced segregation, transmission electron microscopy, molybdenum, rhenium, fission reactor material, compositional redistribution

---

[1]Graduate Student and Scientist, respectively, Materials Science and Technology Division, Argonne National Laboratory, Argonne, IL 60439
[2]Professor, Department of Metallurgy and Mining Engineering, University of Illinos, Urbana, 61801
*Work supported by the U. S. Department of Energy, BES-Materials Sciences, under Contract W-31-109-Eng-38.

Radiation-Induced Segregation and Precipitation in Molybdenum-Rhenium Alloys*

R. A. Erck[1], C. M. Wayman[2] and L. E. Rehn[1]

[1]Materials Science and Technology Division
Argonne National Laboratory
Argonne, IL 60439

[2]Department of Metallurgy and Mining Engineering
University of Illinois
Urbana, IL 61801

Introduction

Due to favorable high temperature mechanical properties, refractory metals and alloys are of interest for structural applications in space-nuclear power systems (1,2). Re additions increase the low temperature ductility of Mo, which otherwise tends to be brittle in the recrystallized condition (3).

Irradiation of an alloy with energetic particles produces interstitial and vacancy point defects which at elevated tempertures may migrate long distances. Fluxes of interstitials and vacancies will be established as these defects migrate to, and annihilate at, point defect sinks such as grain boundaries and the external surface. Any preferential coupling of solute elements to the defect fluxes generated during irradiation will result in enrichment or depletion of solute elements near point defect sinks, i.e. radiation-induced segregation (4,5). Such radiation-induced segregation (RIS) will be an important consideration in evaluating the performance of Mo-Re alloys in elevated temperature irradiation environments.

Other workers have investigated void swelling (6), blistering (7), and microstructural damage (8) in irradiated Mo-Re alloys, but little information on RIS or precipitation has been reported.

*Work supported by the U. S. Department of Energy, BES-Materials Sciences under Contract W-31-109-Eng-38.

Experiment

Molybdenum alloy plates containing 7, 27 and 30 atomic % Re (13, 42, and 45 weight % Re) were kindly provided by F.W. Wiffin of Oak Ridge National Laboratory. Transmission electron microscope (TEM) specimens were punched from ~ 0.25 mm thick foil rolled from this stock. For Rutherford Backscattering Analysis (RBS), rectangular pieces were cut from the ~ 1 mm thick stock. The specimens were solution annealed in vacuum for 5 hours at 1800°C, which resulted in an average grain size of 200 μm. Specimens were sanded with metallurgical papers and electropolished with a 15% sulfuric acid- 5% butyl cellosolve- 80% methanol solution at -50°C.

The irradiations were done at the Argonne National Laboratory Tandem ion irradiation facility. Pressures in the irradiation chamber were in the low 10^{-6} Pa range with an oxygen partial pressure of ~ 10^{-7} Pa. For most experiments, RBS analysis was performed with a 1.0 mm diameter, 1.8 MeV He^{+} beam backscattered at 170° into a ruggedized detector that was cooled with dry ice. Specimens were firmly clamped to a thin Ta holder using Ta tabs, and were heated by an electron beam striking the back of the specimens. Perforations in the Ta holder behind each specimen allowed the specimens to be heated individually. The initial cooling rate of the specimens when the heating was stopped was ~ 100°C/s. Temperatures were measured by means of fine thermocouple wires spotwelded onto each specimen. A temperature gradient (~ 20°C) was noticed across the 10 mm length of the rectangular specimens; this difference in temperature between the irradiated area and the thermocouple was compensated for with the aid of an infrared pyrometer. A furnace controller maintained the specimen temperature within ±2°C during irradiation; the accuracy of an absolute temperature measurement was ±10°C. Because the actual temperature of the specimen was measured, uncertainties due

to beam heating were eliminated.

Defect production profiles and displacement rates were calculated using the TRIM computer code (9). Nominal near-surface displacement rates (ion current density) were calculated to be 1.2×10^{-4}dpa/s (16 $\mu A/cm^2$), and 0.9×10^{-4} dpa/s (12 $\mu A/cm^2$), for Mo-7Re and Mo-30Re, respectively. The projected range of the 1.8 MeV He was ~ 3.5 μm.

Irradiated TEM specimens were electropolished from the back to the irradiated surface with the solution described above. A JEOL 100CX microscope was used for TEM observations. Mo-27Re specimens were employed in the early TEM experiments; later RBS and TEM investigations used only Mo-7Re and Mo-30Re alloys.

Results and Discussion

RBS spectra collected during irradiation of a Mo-7Re specimen at 1250°C are shown in Fig. 1. The time period shown above each spectrum indicates the interval during the irradiation in which the spectrum was collected. Successive increases in the backscattering yield at, and just below, the Re leading edge are apparent as the irradiation proceeds, and show that Re is segregating toward the external surface. The associated reduction in the Mo backscattering yield near the Mo leading edge can also be identified. The amount of Re transported toward the irradiated surface can be determined by taking the difference between successive RBS spectra and the initial spectrum. For this purpose, spectra were first normalized to correct for differences in acquisition times. The normalization procedure consisted of equalizing the RBS yield in a region where no RIS was evident, usually channel numbers 500-600.

In Fig. 2, difference spectra obtained from the RBS spectra in Fig. 1 are shown. Each difference spectrum represents the difference between an RBS spectrum and the (0-5)-minute spectrum. The positive yield, which occurs behind the Re leading edge in the difference spectra, is due to Re enrichment near the surface. Correspondingly, the negative yield behind the Mo edge arises from Mo depletion near the surface. In principle, the integrated difference in the Re enriched region is directly proportional to the amount of Re segregation. In practice, slight variations in incident ion energy produce shifts in elemental leading edges in successive spectra that introduce errors in the conversion of integrated yield to segregation magnitude. For example, in Fig. 1, a shift of 1 channel would introduce an extra $\sim 10^3$ counts at the Re leading edge, and an extra $\sim 4 \times 10^3$ counts at the Mo leading edge. This error can be eliminated by requiring that solute be conserved. Thus an increase in the backscattering yield in the region of Re enrichment must be accompanied by a corresponding decrease in the backscattering yield in the subsurface region, where Re depletion occurs. Because backscattering yields are known, a simple expression can be derived and used to correct the error due to edge shifts. With increasing irradiation temperature, the width of the Re enriched region broadens, and the concentration gradient is reduced. An analytical expression for the steady state point-defect concentration profile in an irradiated solid has been determined by Lam and Rothman (10). The broadening of the Re enriched region arises as a result of the broadening of the point-defect concentration profile at higher temperatures. The integral difference yield described above measures the total amount of Re transported toward the surface, independent of the width of Re enrichment.

The amount of solute enrichment, Y, can be related to the irradiation dose, ϕ, by the expression $Y=a(\phi)^n$. In Ni-Si, for example, n is 0.5 (11), and

and in Cu-Au, n varies with irradiation dose (12). Acquisition of the RBS data occurs linearly in time. Since each difference spectrum represents the average composition change between two different collection periods, the irradiation is representative of that time period, and is different from the average dose when $n \neq 1$. Averback et al (11) have derived a simple expression to determine the effective dose during a collection period as a function of n. To examine the segregation behavior in Mo-Re, integral difference yields were plotted as a function of $(\phi)^n$ for various n, where the effective dose was varied as a function of n. The best mean square fit of the data points to a straight line occurred when n was ~ 0.7 in both alloys. Integral difference yields from irradiations of the Mo-7Re alloy at four different temperatures are shown in Fig. 3, plotted as a function of effective dose to the 0.7 power.

RIS was observed from 800°C to 1500°C in Mo-7Re, and from 850°C to 1225°C in Mo-30Re. The width of the Re-enriched region was significantly broader in the 30% alloy for equivalent irradiation temperatures and doses. Accurate measurements of segregation in Mo-30Re were not possible above 1200°C because the Re enriched region quickly extended below the Mo leading edge. For our experimental conditions, one RBS channel on the abcissa corresponds to a change in specimen depth of 1.4 nm. The dip in the Re yield to the left of the Re enriched region is very slight because the thickness of the Re depletion region is much greater than the thickness of the Re enriched region ($\sim$ 50 nm at the highest dose in Fig. 2).

With the ion beam beam off, some irradiated specimens were annealed at the irradiation temperature for various lengths of time, and then profiled by RBS at room temperature. Thermal back-diffusion of Re away from the enriched surface region occurred, demonstrating that the segregation is indeed a nonequilibrium, radiation-induced phenomenon, and not a radiation-enhanced

approach toward an equilibrium state.

Due to the accumulation of implanted He, small (40 μm diameter) blisters occurred on specimen surfaces at the higher doses and temperatures. However, their appearance produced no noticeable effect on the RBS results.

Precipitation of Chi phase ($MoRe_3$) was observed in Mo-27 and Mo-30Re after irradiation to doses up to 1.5 dpa at temperatures from 750°C to 1075°C. Three varieties of Chi precipitation were identified after irradiation, with a morphology similar in both alloys. At lower temperatures, disk-shaped precipitates, which appeared to have nucleated homogeneously, were seen at the surface. At higher temperatures, Chi formed along grain boundaries and as thin (less than 20nm) precipitates at the irradiated surface. Precipitation was not observed in any irradiated Mo-7Re specimens. Unirradiated specimens of Mo-30Re annealed in quartz capsules for 238 hours at 1000°C, or 73 hours at 1200°C, contained no second-phase precipitates. Figure 4a is a dark field micrograph of Chi phase precipitates with average diameter of 20 nm that formed in a Mo-30Re specimen after a dose of 0.6 dpa at 750°C. Chi precipitates formed with a cube-on-cube crystal orientation with respect to the matrix, i.e., $(100)\|(100)$ and $[010]\|[010]$. Figure 4b is a bright field micrograph of a Mo-27Re specimen that had been irradiated to 0.65 dpa at 950°C, and annealed at ~ 1500°C for 4 seconds. The strong moiré fringes are due to the ~ 2% lattice misfit between Chi and the bcc matrix. The fringes are more or less normal to the operating diffraction vector which is expected for a misfit, but not for a rotation moiré pattern (13). The irregular fringe spacing indicates that a number of dislocations are present; an example is circled. Micrographs of a precipitate that had a very regular fringe spacing revealed that the fringe spacing varied with equivalent diffraction vectors, and contained a second set of less dominant fringes, indicating that one or

two sets of interface dislocations were present. The thickness of the precipitates in Fig. 4b is estimated to be less then 20nm by means of stereo microscopy.

Figure 4c is a bright field micrograph of a grain boundary triple point in a Mo-30Re specimen irradiated at 1000°C to 1.3 dpa. Heavy Chi precipitation is seen coating the grain boundaries. When Chi precipitate free of bcc matrix was imaged, no inversion domains (14), anti-phase boundaries or super-dislocations were found (15).

Figure 4d is a dark field micrograph of a Mo-27Re specimen irradiated to 0.65 dpa at 1000°C. Tilting revealed that the closely spaced fringes perpendicular to the diffraction vector are moiré fringes and that some of the fringes are due to interface dislocations. This suggests that the precipitate is forming semi-coherently on the underlying bcc matrix. The small, barely visible precipitation may be Mo_2C, which was observed in some foils.

Large precipitates, as seen in figures 4b, c, and d, can be resolved with the optical microscope. Such precipitation is restricted to the irradiated area. Precipitates are often triangular in shape, which may be due to the relative ease of precipitate growth along certain crystallographic directions. The initial rolling of the foil preferentially oriented {111} planes parallel to the foil surface.

A specimen similar to that in Fig. 4c was sectioned by electro-polishing. In the near surface region (less than 100 nm) no dislocations, loops or cavities were found for doses up to 1.6 dpa. Removal of ~ 200nm of material completely eliminated the surface precipitates and reduced the apparent density of grain boundary precipitates. At a section depth of 2 μm, only small (~ 5nm diameter) He bubbles and dislocations were seen.

Irradiation of Mo-27Re at 1050°C to 0.6 dpa and annealing at the same temperature for 45 minutes resulted in the formation of a number of irregularly shaped colonies, containing up to several hundred individual Chi precipitates (Figure 5a). A large number of superlattice spots can be seen in the selected area diffraction pattern (Figure 5b). As was mentioned above, Chi phase precipitates form with a cube-on-cube orientation with respect to the bcc matrix. Superlattice spots from precipitates with this orientation are shown in Fig. 5b; the superlattice spots are connected by solid lines. Two other orientations of recriprocal lattice spots can be identified (dashed lines). These orientations can be described in terms of a reflection of the cube-on-cube Chi orientation across {111} planes, i.e., a growth twin orientation. Precipitates imaged by using one of the superlattice spots are shown in Fig. 5c. The moiré fringes arise from the higher order superlattice spots that are coincident with the bcc diffraction spots. Dark field images were obtained using superlattice spots from a number of zone-axis patterns. Superlattice spots which image more than one orientation (arrow in Fig. 5b) were avoided. When the superlattice spots were indexed in a consistent manner, and the dark field micrographs examined, it was possible to associate each precipitate with a twin or cube-on-cube orientation. All four possible {111} twin orientations and the cube-on-cube orientation were represented. Each precipitate could be associated with one unique crystallographic orientation. Precipitates with twin orientations were occasionally observed in other specimens, but the cube-on-cube orientation was more common.

Rhenium is an undersize solute (16), and diffuses faster than molybdenum (17), in solid solution Mo-Re alloys. Preferential exchange of Re atoms with migrating vacancies would result in transport of Re in a direction opposite to that of the defect fluxes, i.e., away from the external surface. The Re

enrichment that is observed is thought to be due to segregation occurring primarily via an interstitial mechanism: undersize solutes are more readily accomodated in interstitial sites and therefore are expected to be preferentially transported toward sinks. The enrichment is in agreement with the size-effect correlation first noticed by Okamoto and Wiedersich (18).

The precipitation of Chi phase at the irradiated surface where RIS is seen suggests that the Re rich second phase forms when the local solubility limit is exceeded. The redistribution of solute to form large precipitates may be aided by surface diffusion. The precipitation seen at the lower temperatures is similar to the homogeneous, irradiation induced precipitation described by Cauvin and Martin (19), but differs in its being a surface, not bulk, phenomenon. The smaller size of the precipitates can be attributed to a higher nucleation rate and/or to a lower growth rate at lower temperatures.

Conclusion

The experimental results show that radiation-induced segregation and precipitation occur at elevated temperatures in irradiated Mo-Re alloys. Segregation can be explained by defect-flux driven transport of Re to point defect sinks by means of an intersititial mechanism. Precipitation occurs when the local solute solubility limit is exceeded. Because physical and mechanical properties of alloys depend sensitively on alloy composition, this RIS is expected to be an important consideration in evaluating the suitability of Mo-Re alloys in elevated temperature irradiation environments.

Acknowledgment

The authors would like to thank P. M. Baldo for valuable assistance with the irradiations. This work is supported by the U. S. Department of Energy.

References

1. Proceedings of the Symposium on Refractory Alloy Technology for Space Nuclear Power Applications, Cooper, R. H. and Hoffman, E. E., (Eds.), Oak Ridge, TN, Aug. 10-11, 1983, NTIS Report No. CONF-8308130 (January 1984).

2. Space Nuclear Power Systems 1984, El-Genk, M. S., and Hoover, M. D. (Eds.), Orbit Book Company, Malabar, FL, 1985.

3. Lundberg, L. B., Ohriner, E. K. Tuominen, S. M., Whelan, E. P., and Shields, Jr., J. A., Proceedings of the AMAX Symposium on Physical Metallurgy and Technology of Molybdenum and Its Alloys, Miska, K. H., Semchyshen, M., Whelan, E. P. (Eds.), Oct. 29-30, 1984, Ann Arbor, MI, pp. 71-79.

4. Rehn, L. E. and Okamoto, P. R. in Phase Transformations During Irradiation, F. C. Nolfi, Jr., Ed., Applied Science Publishers, Barking, England, 1983, pp. 247-290

5. Wiedersich, H., Okamoto, P. R., and Lam, N. Q., Journal of Nuclear Materials, Vol. 83, 1979, pp. 98-108.

6. Igata, N., Kohyama, A., and Nomura, S., Journal of Nuclear Materials, Vol. 103 & 104, 1981, pp.1157-1162.

7. Igata, N., and Kohyama, A. in Proceedings of the Fourth Topical Meeting of The Technology of Controlled Nuclear Fusion, Oct 14-17, 1980, King of Prussia, PA, NTIS Report No. CONF-801011 (July 1981), pp.1673-1682.

8. Rau, R. C., Moteff, J., and Ladd, R. L., Journal of Nuclear Materials, Vol. 40, 1971, pp. 233-235.

9. Biersack, J. P., and Haggmark, L. G., Nuclear Instruments and Methods, Vol. 174, 1980, pp. 257-269.

10. Lam, N. Q., and Rothman, S. J., Radiation Effects, Vol. 23, 1974, pp. 53-59.

11. Averback, R. S., Rehn, L. E., Wagner, W., Wiedersich, H., and Okamoto, P. R., Physical Review B, Vol. 28, No. 6, 15 Sept. 1983, pp. 3100-3109.

12. Hashimoto, T. Rehn, L. E., and Okamoto, P. R., Radiation Induced Precipitation in Cu-Au Alloys, Published in this volume.

13. Edington, J. W., Practical Electron Microscopy in Materials Science, Van Nostrand Reinhold, New York, 1976.

14. Snykers, M., Serneels, R., Delavignette, P., Gevers, R., and Amelinckx, S., Crystal Lattice Defects, Vol. 3, 1972, pp. 99-101.

15. Meulemans, M., Delavignette, P., Garcia-Gonzales, F., and Amelinckx, S., Materials Research Bulletin, Vol. 5, 1970, pp. 1025-1030.

16. King, H. W., Journal of Materials Science, Vol. 1, 1966, pp. 79-90.

17. Savitskii, E. M., Tylkina, M. A., and Povarova, K. B., Rhenium Alloys, Israel program for Scientific Translations, Jerusalum, 1970.

18. Okamoto, P. R., and Wiedersich, H., Journal of Nuclear Materials, Vol. 53, 1974, pp. 336-345.

19. Cauvin, R., and Martin, G., Journal of Nuclear Materials, Vol. 83, 1979, pp. 67-78.

Figure Captions

Figure 1- Series of RBS spectra collected during a 1.8 MeV He irradiation of a Mo-7Re specimen at 1250°C.

Figure 2- Difference spectra for the RBS spectra in Fig. 1.

Figure 3- Integral difference yields as a function of dose to the 0.7 power for Mo-7Re specimens irradiated at 900°C, 1150°C, 1250°C, and 1450°C.

Figure 4- TEM micrographs: (a) Mo-30Re specimen irradiated to 0.6 dpa at 750°C. Dark field, using a Chi superlattice spot. (b) Mo-27Re specimen irradiated to 0.65 dpa at 950°C, and annealed at ~ 1500°C for 5 s. Bright field. (c) Mo-30Re specimen irradiated to 1.3 dpa at 1000°C. Bright field. (d) Mo-27Re specimen irradiated to 0.65 dpa at 1000°C. Dark field, using a Chi superlattice spot.

Figure 5- Mo-27Re specimen irradiated to 0.6 dpa at 1050°C and annealed for 45 minutes at the irradiation temperature. (a) Bright field micrograph. (b) Selected area diffraction pattern. The arrow points to a superlattice spot arising from more than one precipitate orientation. (c) Dark field micrograph of same area as in (a). The precipitates seen are associated with only one twin orientation.

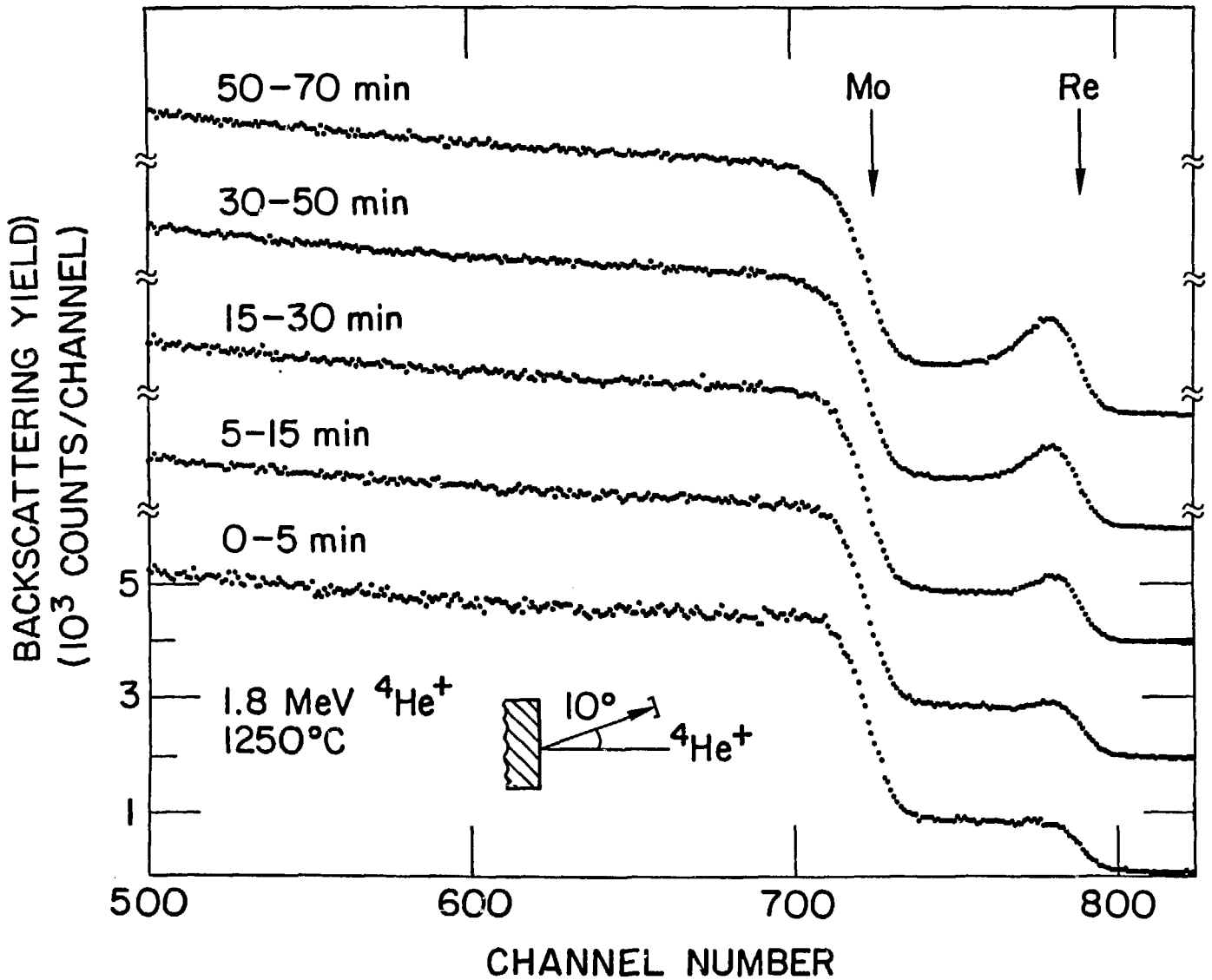
50–70 min
30–50 min
15–30 min
5–15 min
0–5 min
Mo
Re
1.8 MeV $^4He^+$
1250°C
10°
$^4He^+$
BACKSCATTERING YIELD
(10^3 COUNTS/CHANNEL)
5
3
1
500
600
700
800
CHANNEL NUMBER

Fig-1

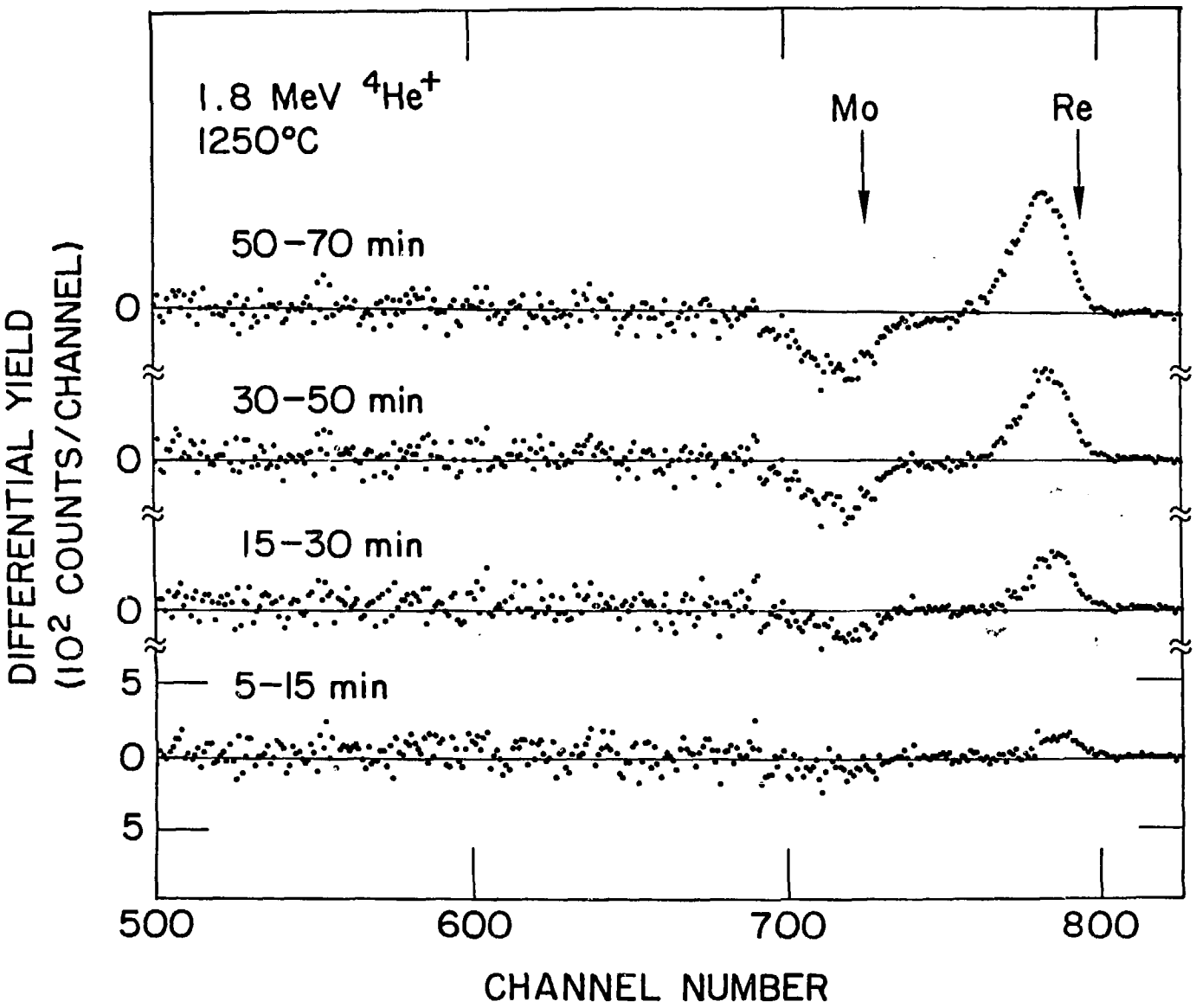
1.8 MeV $^4He^+$
1250°C
Mo
Re
50–70 min
30–50 min
15–30 min
5–15 min
0
0
0
5
0
5
DIFFERENTIAL YIELD
(10^2 COUNTS/CHANNEL)
500
600
700
800
CHANNEL NUMBER

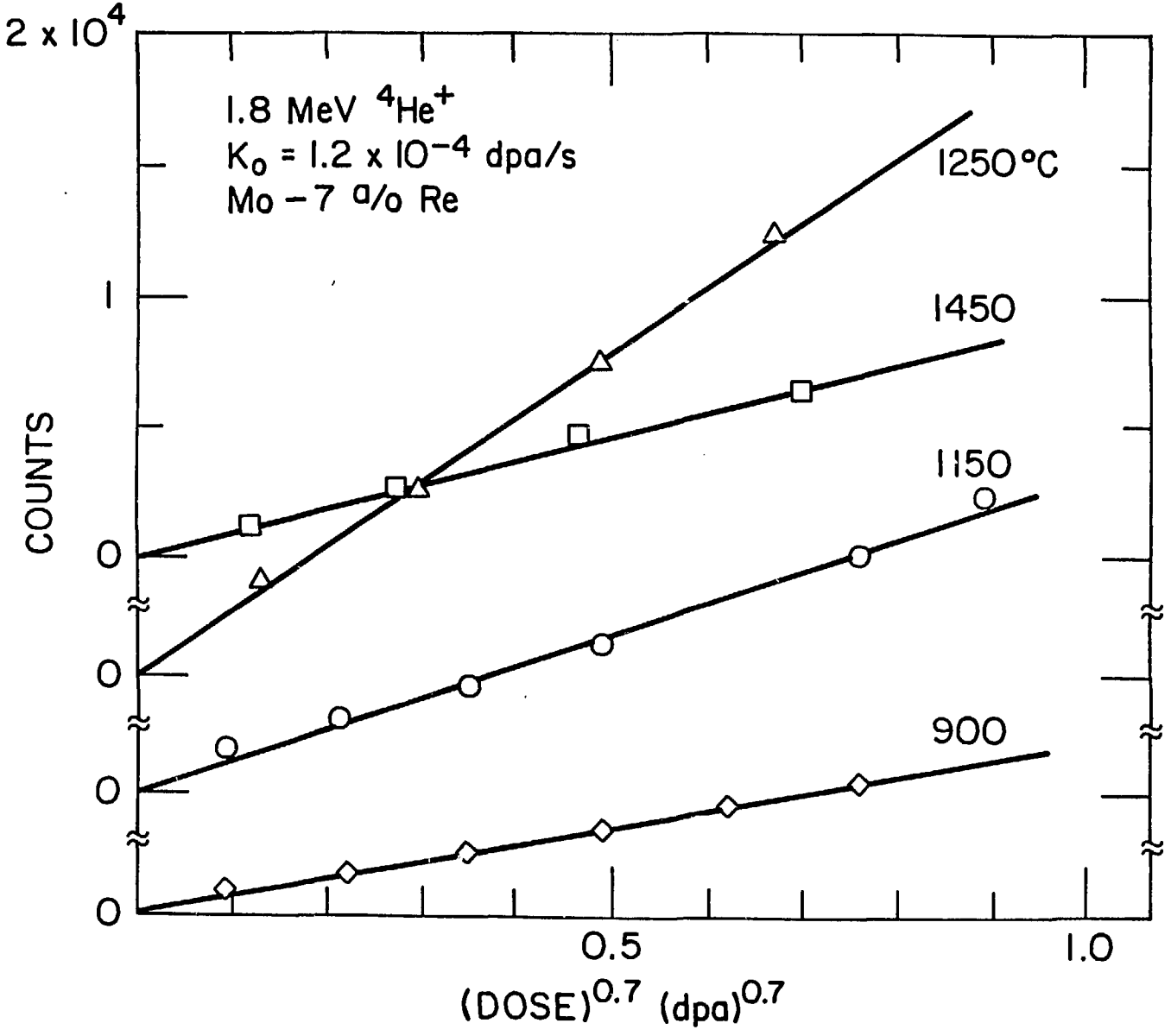
2 x 10^4
1.8 MeV 4He+
K0 = 1.2 x 10^-4 dpa/s
Mo – 7 a/o Re
1250°C
1450
1150
900
COUNTS
1
0
0
0
0.5
1.0
(DOSE)^0.7 (dpa)^0.7

Fig 2

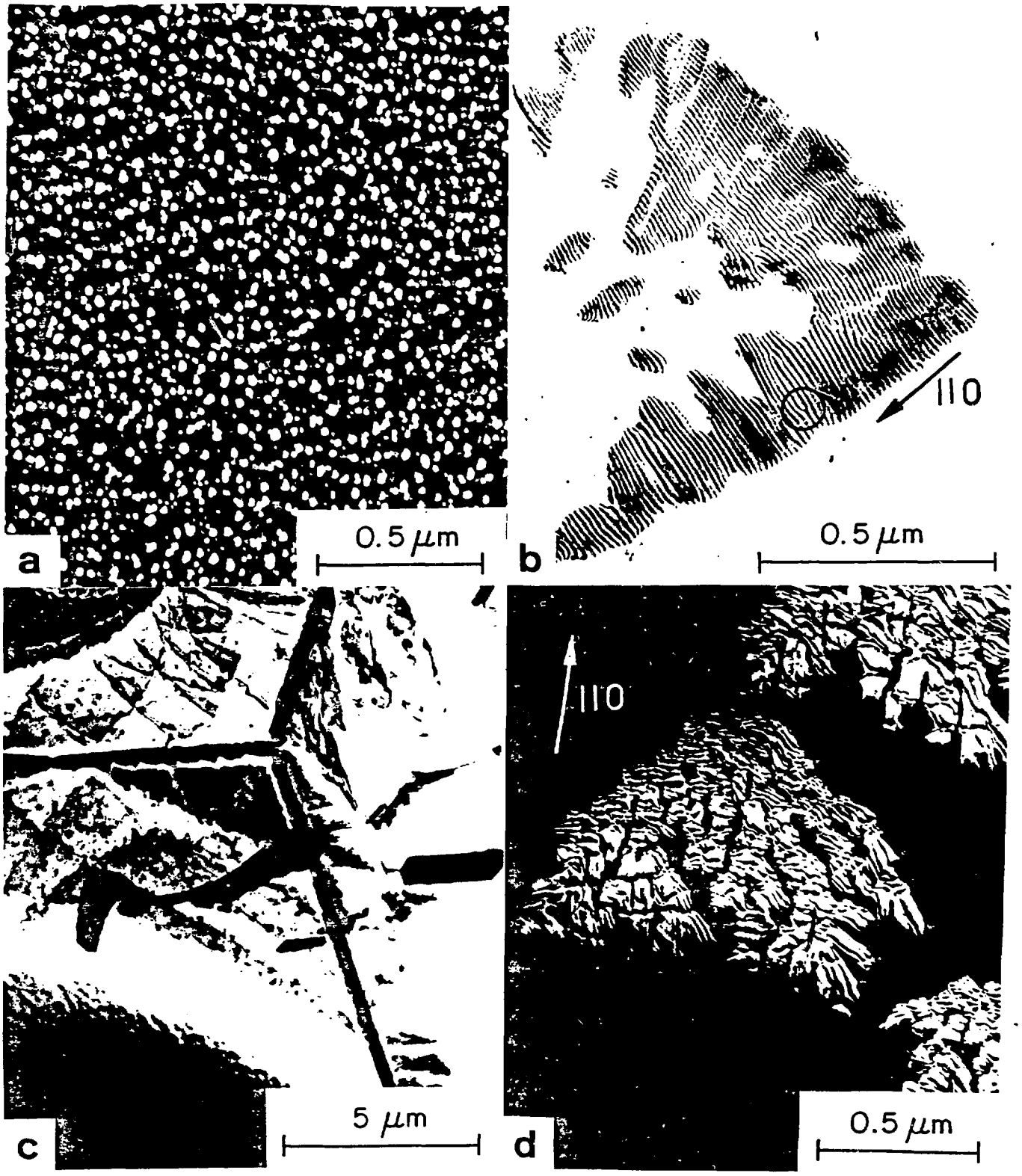

Fig 4

a
1 μm
b
c